Complex-Forming Bimolecular Reactions of Metastable NH($a^1\Delta$) with $H_2O(\tilde{X}^1A_1)$ and $H_2O_2(\tilde{X}^1A)$

W. Hack and R. Jordan

Max-Planck-Institut für Strömungsforschung, Bunsenstraße 10, D-37073 Göttingen, Germany

Key Words: Chemical Kinetics / Elementary Reactions / Energy Transfer / Molecular Interactions / Photochemistry

The elementary reactions:

$NH(a^1\Delta) + H_2O(\tilde{X}) \rightarrow$ products (1)

and

$NH(a^1\Delta, v) + H_2O_2(\tilde{X}) \rightarrow$ products (2)

were studied in a quasistatic laser photolysis cell at a pressure of 20 mbar in the temperature range $295 \leq T/K \leq 523$ and at room temperature respectively. $NH(a^1\Delta, v)$ was produced by excimer laser photolysis of $HN_3(\tilde{X})$ and detected by laser-induced fluorescence (LIF). A variable delay time between photolysis and detection pulse brought about the time resolution. The NH(a) depletion yielded the following rate constants:

$k_1(T) = (3.5 \pm 0.8)\,10^{13}\,(T/295\ K)^{-(1.5\pm0.2)}\ cm^3/mol\ s$

$k_2(v = 0) = (7.5 \pm 1.4)\,10^{13}\ cm^3/mol\ s$

$k_2(v = 1) = (7.1 \pm 0.9)\,10^{13}\ cm^3/mol\ s$

The reaction products of reaction (1) are $NH_2(\tilde{X}) + OH(X)$. For reaction (2) $NH_2(\tilde{X})$ radicals were detected (24%); the quenching channel was found to be unimportant $k_q < 7.5 \cdot 10^{11}\ cm^3/mol\ s$. The reaction mechanism is discussed. The reaction $NH(a) + H_2O(\tilde{X})$ is compared to the reaction $NH(X) + H_2O(\tilde{X})$.

Introduction

The reactions of electronically excited singlet atoms and molecules can be used to produce electronic chemically activated complexes. Electronically excited oxygen atoms for example react with methane:

$$O(^1D) + CH_4 \rightarrow CH_3OH(\tilde{X})^{\#} \rightarrow CH_2(\tilde{a}^1A_1) + H_2O$$

and produce the vibrationally excited methanol in the electronic ground state i.e. the initial electronic excitation energy and the energy resulting from the broken and formed chemical bonds are available in the electronic chemically activated methanol. A minor product channel in this reaction is $CH_2(\tilde{a}^1A_1) + H_2O(\tilde{X})$. As the reverse reaction, given above, electronic chemically activated methanol can be formed in the reaction of $CH_2(\tilde{a})$ and H_2O; whereas the reverse reactions of the main products $OH(X^2\Pi) + CH_3(\tilde{X}^2A_2'')$ form chemically activated methanol in a combination reaction of two doublet radicals.

The reaction of the imino radical $NH(a^1\Delta)$ with water leads to an electronic chemically activated hydroxylamine complex:

$$NH(a^1\Delta) + H_2O(\tilde{X}^1A_1) \rightarrow NH_2-OH(\tilde{X})^{\#} \rightarrow \text{products} \quad (1)$$

It is a fast process at room temperature i.e. the rate coefficient is near gas kinetic collison number. The amino radical in the electronic ground state $NH(X^3\Sigma^-)$ reacts with H_2O at high temperatures as observed in shock waves [1]. Extrapolating the high temperature data with the experimentally determined activation energy to low temperatures leads to a very low room temperature rate constant for that reaction. The difference in the reaction dynamics of NH(a) and NH(X) with H_2O should be observed in the temperature dependence of the rate coefficient if the activation barrier to form the $NH_2OH(\tilde{X})^{\#}$ complex is small. The potential energy surface for the reaction was studied by *ab initio* molecular orbital theory [2, 3] with essentially no barrier to form a primary $NH\cdots OH_2$ donor acceptor complex which isomerizes to the more stable NH_2OH. In the liquid phase, when HN_3 was photolyzed in $H_2O(l)$ the $NH_2OH(\tilde{X})^{\#}$ is quenched and hydroxylamine was found as the main reaction product [4].

NH(a) and ND(a) react with H_2O at room temperature with nearly the same rate [5] whereas D_2O is significantly less reactive towards NH(a) and ND(a) than H_2O [5]; indicating that an insertion into the O – H respectively O – D bond takes place. In these studies no indication for an efficient exchange reaction:

$$NH(D)(^1\Delta) + H_2(D_2)O(\tilde{X}) \rightleftarrows ND(H)(^1\Delta) + H(D)H(D)O(\tilde{X})$$

was observed in agreement with the PES which predict the barrier for the insertion but not for the formation of primary $HN\cdots OH_2$ complex.

  0005-9021/97/0303-0545 $ 15.00+.25/0

The reaction of NH(a) with hydrogenperoxide:

$$NH(a^1\Delta) + H_2O_2 \rightarrow \text{products} \quad (2)$$

which might show a similar reaction dynamics as H_2O has, to our knowledge, not yet been studied directly neither experimentally nor theoretically.

The aim of this study is to ensure the complex formation reaction dynamics for reaction (1) by following the temperature dependence of the reaction rate coefficient. The reaction (2) is to be studied with respect to the reaction rate at room temperature and the reaction products.

2. Experimental

The experiments were performed in a quasistatic (i.e. the flow is negligible on the time scale of the duration between pump and probe laser, but sufficient to exchange the gas volume between two subsequent pump pulses) laser photolysis/laser induced fluorescence (LIF) system. The experimental set up is described in detail elsewhere [6]. The carrier gas is He at a total pressure of 20 mbar. An inner cylinder, which was inserted into the fluorescence cell, was heated in the temperature range $295 \leq T/K \leq 523$. The temperature was controlled ± 1 K.

The photolysis laser was an KrF-exciplex laser (LPX 205 Lambda Physik) with pulse energies in the range $200 \leq E/mJ \leq 400$ and a beam area of about 180 mm^2. The probe laser was an exciplex laser (LPX 205 Lambda Physik XeCl; $230 \leq E/mJ \leq 290$) pumped dye laser (FL 3002 Lambda Physik) with fluence in the range $20 \leq E/mJ\ cm^{-2} \leq 220$ and a beam area of $\approx 9\ mm^2$. This fluence was proved to be sufficient to saturate the excited transition. The frequency-doubled dye laser beam with a fluence of $2 \leq E/mJ\ cm^{-2} \leq 3$ was sufficient to saturate the observed transition in OH (see below).

The NH(a) radicals were produced in the $HN_3(\tilde{A}\text{-}\tilde{X})$ photolysis at $\lambda = 248$ nm in the vibronic states $v = 0$ and 1, at rotational temperatures, significantly above room temperature. The rotational distribution relaxes at the given experimental conditions within the first μs to a nearly room temperature distribution mainly in collisions with He. If the mixture of HN_3 and H_2O_2 was photolyzed also $OH(X^2\Pi)$ radicals are formed. They were detected with the $Q_1(1)$ line of the $A^2\Sigma^+$, $v = 0 \leftarrow X^2\Pi\ v = 0$ transition at $\lambda = 307.85$ nm. NH(a, $v = 0$) was detected with the transition $c^1\Pi$, $v' = 0 \leftarrow a^1\Delta\ v'' = 0$, excited in the wavelength range $325 \leq \lambda/nm \leq 328$. The undispersed fluorescence from the excited state was observed perpendicular to the laser beam. NH(a, $v = 1$) was excited via the transition $c^1\Pi$, $v' = 1 \leftarrow a^1\Delta\ v'' = 1$ in the wavelength range $336 \leq \lambda/nm \leq 340$, and the undispersed fluorescence was detected. Filters were used to suppress scattered radiation of the excitation beam. The transition $A^3\Pi\ v' = 0 \leftarrow X^3\Sigma,\ v'' = 0$ was excited in the wavelength range $335.5 \leq \lambda/nm \leq 338.5$ in order to detect NH(X) by the fluorescence of the $A^3\Pi\ v' = 0$ state.

The $NH_2(\tilde{X}^2B_1)$ radicals were detected by the fluorescence induced via the transition $\tilde{A}^2A_1(090) \leftarrow \tilde{X}^2B_1(000)$ at a wavelength $\lambda = 597.65$ nm.

Gases with the highest commercially available purity were used (He 99.9999% Praxair). HN_3 was produced by melting stearic acid $CH_3(CH_2)_{16}COOH$ with NaN_3 and dried with $CaCl_2$. HN_3 was stored in a bulb at a pressure of $p(HN_3) \leq 200$ mbar, diluted with He to one atmosphere.

The H_2O_2 (commercially available at 85% (Solvay Interox)) was enriched to 99%. Its concentration was determined via $KMnO_4$ titration. H_2O_2 was added to the He gas stream in a one-stage saturator. The H_2O_2 concentrations in the cell were measured by pumping the gas stream through a $N_2(l)$ trap in front of the cell and determine the amount of H_2O_2 trapped in a given time by titration.

2. Results

The elementary reaction:

$$NH(a^1\Delta, v = 0) + H_2O(\tilde{X}) \rightarrow \text{products} \quad (1)$$

was followed by the NH(a, $v = 0$) depletion in the presence of a large excess of $[H_2O]$ over [NH(a)], i.e. $7 \cdot 10^3 \leq [H_2O]_0/[NH(a)]_0 \leq 1 \cdot 10^5$. The pseudo first order rate coefficients $k_1'(T)$ are shown in Fig. 1 for four different temperatures in the range $295 \leq T/K \leq 523$. The experimental conditions are summarized in Table 1. The intercept in Fig. 1 is due to the NH(a) depletion by HN_3:

$$NH(a) + HN_3 \rightarrow \text{products} \quad (3)$$

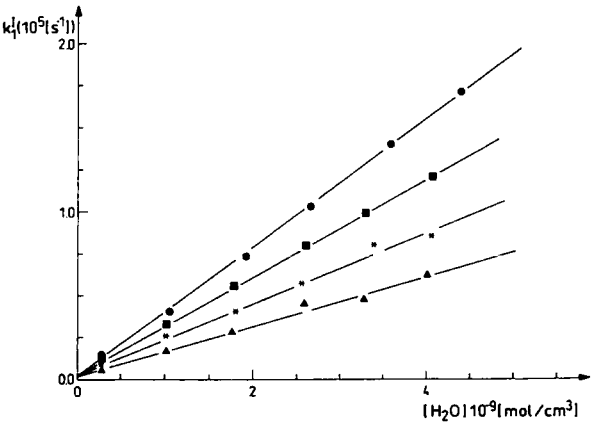

Fig. 1
First order rate coefficients k_1' as a function of the H_2O concentration at various temperatures: ● $T = 295$ K; ■ $T = 346$ K; * $T = 416$ K; ▲ $T = 523$ K

The slope of the k_1' vs. $[H_2O]_0$ plot was used to determine the second order rate constant $k_1(T)$ as given in Table 1. The rate coefficient k_1 decreases with increasing temperature. The temperature dependence of k_1 is shown in Fig. 2. Included are also the room temperature rate data published in the literature (see Discussion).

Table 1
Experimental conditions for the determination of the rate coefficient $k_1(T)$

T / K	P / mbar	$[HN_3]$ / 10^{-11} mol cm^{-3}	$[H_2O]$ / 10^{-9} mol cm^{-3}	k_1' / 10^4 s^{-1}	$k_1(T)$ / cm^3 mol^{-1} s^{-1}
295	20	3	0.0	0.24	$(3.8\pm0.8)\cdot10^{13}$
295	20	3	0.3	1.38	
295	20	3	1.1	3.94	
295	20	3	1.9	7.28	
295	20	3	2.7	10.3	
295	20	3	3.6	14.0	
295	20	3	4.4	17.2	
346	20	3	0.0	0.17	$(2.9\pm0.6)\cdot10^{13}$
346	20	3	0.3	1.13	
346	20	3	1.0	3.28	
346	20	3	1.8	5.57	
346	20	3	2.6	7.96	
346	20	3	3.3	9.88	
346	20	3	4.1	12.1	
416	20	3	0.0	0.15	$(2.1\pm0.9)\cdot10^{13}$
416	20	3	0.3	0.90	
416	20	3	1.0	2.55	
416	20	3	1.8	3.99	
416	20	3	2.6	5.66	
416	20	3	3.4	7.94	
416	20	3	4.1	8.54	
523	20	3	0.0	0.82	$(1.5\pm0.8)\cdot10^{13}$
523	20	3	0.3	5.83	
523	20	3	1.0	1.62	
523	20	3	1.7	2.69	
523	20	3	2.6	4.45	
523	20	3	3.3	4.72	
523	20	3	4.0	6.19	

The rate coefficient is represented by:

$$k_1(T) = (3.5\pm0.8)^{13}\cdot(T/295\text{ K})^{-1.5\pm0.2}\text{ cm}^3/\text{mol s}$$

in the above given temperature range. The errors are estimated from the standard deviation obtained from the single measurements and the uncertainties of the measured experimental parameters. As the main product $NH_2(\tilde{X})$ was confirmed.

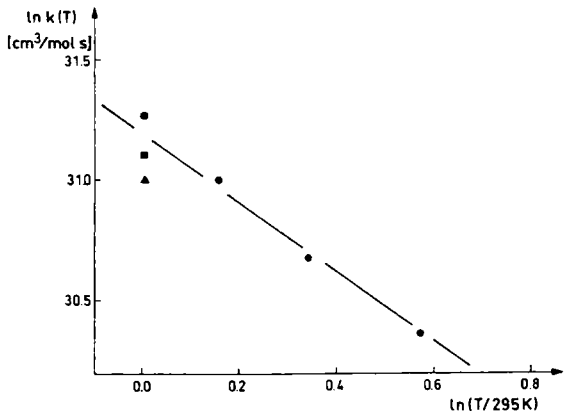

Fig. 2
Rate coefficient $k_1(T)$ as a function of T ● – – ● – – this work (measured points). ■ Ref. [5]; ▲ Ref. [13]

The rate coefficients of the reactions:

$$NH(a, v=0) + H_2O_2 \rightarrow \text{products} \quad (2')$$

and

$$NH(a, v=1) + H_2O_2 \rightarrow \text{products} \quad (2'')$$

were measured at room temperature. The decay of $NH(a, v=0)$ and $NH(a, v=1)$ was determined in independent experiments. Hydrogenperoxide was applied in large excess over NH(a) in the range $2\cdot10^4 \le [H_2O_2]_0/[NH(a,0)]_0 \le 2\cdot10^5$. The initial concentration of $NH(a, v=1)$ was always smaller than the initial concentration of $NH(a, v=0)$ and thus the excess ratio for $NH(a, v=1)$ was larger than the above given range. Hydrogenperoxide is photolyzed at $\lambda = 248$ nm due to $H_2O_2 \xrightarrow{h\nu\,(248\text{ nm})} 2\,OH(X)$. The quantum yield for OH production from 248 nm photolysis of H_2O_2 was determined to be $\Phi_{248\text{ nm}} = 1.58$ [7]. Photolysis products other than OH are not observed. *Ab initio* calculations predict the O – O bond as the dissociative coordinate [8]; thus it can be assumed that OH is the only product of the H_2O_2 photolysis. If there is a further photolytic dissociation channel $H_2O_2 \rightarrow HO_2 + H$ the initial H atom concentration would be not higher than the range $0.7 \le [H]\ 10^{-12}$ mol cm$^{-3} \le 6$ and too small to influence the NH(a) concentration profiles. HO_2 is

present in the system anyhow as the product of the reaction $OH + H_2O_2$ (see below). The initial OH(X) concentration was estimated to be in the range $0.5 \leq [OH]_0\ 10^{-11}$ mol $cm^{-3} \leq 4.6$. The initial OH concentration varied with the H_2O_2 concentration but was also varied independent of $[H_2O_2]_0$ by varying the photolysis laser fluence. In such independent experiments a rate coefficient of the reaction:

$$NH(a) + OH \rightarrow \text{products} \quad (4)$$

was determined [9, 10]. A very fast rate of k_4 (295 K) = $(7.5 \pm 2) \cdot 10^{14}$ cm^3/mol s was estimated [9, 10].

The OH is mainly depleted in the reaction:

$$OH(X) + H_2O_2 \rightarrow H_2O + HO_2 \quad (5)$$

with a rate $k_5 = 1.0 \cdot 10^{12}$ cm^3/mol s [11]. Also the reaction:

$$OH(X) + HN_3 \rightarrow \text{products} \quad (6)$$

contribute to the OH depletion in the system. The rate of this reaction was determined in independent experiments. At room temperature a rate coefficient k_6(295 K) = $7.7 \cdot 10^{12}$ cm^3/mol s was measured [9, 10]. This rate coefficient was inserted to calculate the OH concentration profiles under the experimental conditions applied, and to predict the effect of reaction (4) on [NH(a)](t). At short reaction times the NH(a) depletion by OH via reaction (4) is about 10% of the NH(a) depletion by H_2O_2. At longer reaction times the influence of reaction (4) on the NH(a) profile is marginal since OH is consumed in reactions (5) and (6). Although the influence of OH on the NH(a) concentration profile is different for different reaction times, no deviation from linearity in the $\ln\{[NH(a)](t)/[NH(a)]_0\}$ vs. time-plot was observed as shown in Fig. 3. In a plot of the observed first order rate constant (k'_2) against the photolysis laser energy (E) a slight increase of k'_2 (E) with E was observed. Extrapolating to $E = 0$ i.e. to $[OH]_0 = 0$ results in a correction for k'_2 in the order of 10% due to the effect of OH radicals. This correction is taken into account in the first order rate coefficients given in Table 2.

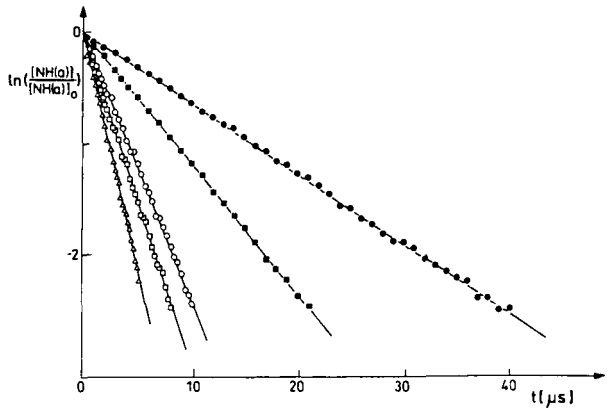

Fig. 3
Concentration profile of NH(a, $v = 0$) in the presents of various H_2O_2 concentrations.
● $[H_2O_2]_0 = 0.7 \cdot 10^{-9}$ mol/cm^3; ■ $[H_2O_2]_0 = 1.4 \cdot 10^{-9}$ mol/cm^3;
○ $[H_2O_2]_0 = 2.8 \cdot 10^{-9}$ mol/cm^3; □ $[H_2O_2]_0 = 3.6 \cdot 10^{-9}$ mol/cm^3;
△ $[H_2O_2]_0 = 5.0 \cdot 10^{-10}$ mol/cm^3

The results obtained for the first order rate constant, k'_2, as a function of $[H_2O_2]_0$ are presented in Fig. 4. A straight line is observed which strikes the origin. The contribution of the reaction (3) is too small to be of any significance. The second order rate constant obtained from the slope of the $k'_2([H_2O_2])$ vs. $[H_2O_2]$ plot in Fig. 4 is:

$$k'_2(v = 0) = (7.5 \pm 1.4)\ 10^{13}\ cm^3/\text{mol s}\ .$$

The errors are estimated from the standard deviation and the uncertainties of the measured experimental parameters, in particular the H_2O_2 concentration in the reaction volume.

Table 2
Experimental conditions for determining k_2 for NH(a, $v = 0$, 1)

	T / K	p_{ges} / mbar	$[HN_3]$ / 10^{-11} mol cm^{-3}	$[H_2O_2]$ / 10^{-9} mol cm^{-3}	k'_2 / 10^5 s^{-1}
NH(a, $v = 0$)	295	20	2.2	0.7	0.54
	295	20	2.2	1.4	1.04
	295	20	2.2	2.1	1.56
	295	20	2.2	2.8	2.12
	295	20	2.2	3.6	2.63
	295	20	2.2	4.3	3.19
	295	20	2.2	5.0	3.80
	295	20	2.2	5.8	4.29
NH($v = 1$)	295	20	2.2	0.7	0.50
	295	20	2.2	1.4	1.02
	295	20	2.2	2.1	1.48
	295	20	2.2	2.8	2.02
	295	20	2.2	3.6	2.53
	295	20	2.2	4.3	3.02
	295	20	2.2	5.0	3.39
	295	20	2.2	5.8	4.25

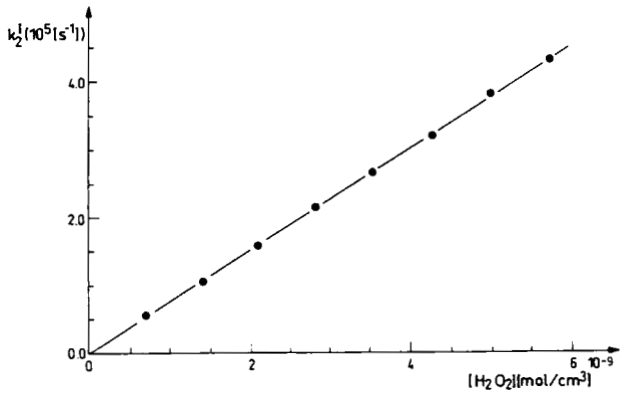

Fig. 4
First order rate coefficient concentration versus $[H_2O_2]$ for the reaction NH(a, $v = 0$) + H_2O_2 → products (2)

For the vibronic excited NH(a), i.e. NH(a, $v = 1$), a rate coefficient,

$$k_2''(v = 1) = (7.1 \pm 0.9)\, 10^{13}\ \mathrm{cm^3/mol\ s}\ ,$$

was determined in the same way from the measured NH(a, $v = 1$) concentration profiles. From the concentration profiles of NH(a, $v = 0$) no indication was found that vibrational deact. activation,

$$\mathrm{NH(a}, v = 1) + H_2O_2 \rightarrow \mathrm{NH(a}, v = 0) + H_2O_2\ ,$$

is of any importance. The relative values of k_2' and k_2'' point in the same direction (see Discussion).

The reaction products of reaction (2) were studied with respect to quenching:

$$\mathrm{NH(a)} + H_2O_2 \rightarrow \mathrm{NH(X)} + H_2O_2 \qquad (2q)$$

and with respect to $NH_2(\tilde{X})$ formation:

$$\mathrm{NH(a)} + H_2O_2 \rightarrow NH_2(\tilde{X}\,^2B_1) + HO_2(\tilde{X}) \qquad (2a)$$

For the quenching channel the NH(X) yield in reaction (2) was compared with the NH(X) yields in the reaction:

$$\mathrm{NH(a)} + N_2(X) \rightarrow \mathrm{NH(X)} + N_2(X) \qquad (7)$$

which deactivates NH(a) with a rate of $k_7 = 5 \cdot 10^{10}\ \mathrm{cm^3/mol\ s}$ [12]. The quenching channel was found to be unimportant, i.e. 0.7% of the initial $[\mathrm{NH(a)}]_0$ appears as NH(X) product. This leads to a value of $k_q(295\ \mathrm{K}) = 5 \cdot 10^{11}\ \mathrm{cm^3/mol\ s}$.

The reference reaction used for the calibration of $NH_2(\tilde{X})$ was:

$$\mathrm{NH(a)} + H_2O \rightarrow NH_2(\tilde{X}\,^2B_1) + \mathrm{OH}(X\,^2\Pi) \qquad (8)$$

In this reaction the formation of $NH_2(\tilde{X}\,^2B_1)$ is known to be 90% of the [NH(a)] inserted [13]. The $NH_2(\tilde{X})$ concentration profile obtained in reaction (2) was simulated taking into account the $NH_2(\tilde{X})$ formation in reaction (3)

$$\mathrm{NH(a)} + HN_3 \rightarrow NH_2(\tilde{X}, \tilde{A}) + N_3 \qquad (3a)$$

and the depletion in the reaction:

$$NH_2(\tilde{X}) + H_2O_2 \rightarrow \text{products} \qquad (8)$$

From the corrected maximum in the $[NH_2(\tilde{X})]$ profile it was determined that the formation of $NH_2(\tilde{X})$ contributes 24% to the depletion of NH(a) in reaction (2) i.e. $k_{2a}(295\ \mathrm{K}) = 1.8 \cdot 10^{13}\ \mathrm{cm^3/mol\ s}$.

The formation of OH was not observed due to the large amount of OH present in the system from the H_2O_2 photolysis.

Discussion

The reaction

$$\mathrm{NH(a\,^1\Delta)} + H_2O(\tilde{X} \rightarrow NH_2(\tilde{X}) + \mathrm{OH(X)} \qquad (1)$$
$$\Delta_R H = -57.5\ \mathrm{kJ/mol}$$

has been studied at room temperature. The values for the rate coefficients obtained with very similar experimental conditions are included in Fig. 2 and are in agreement with the room temperature value obtained in this work. The temperature dependence has not yet been measured directly. The negative temperature dependence represented with:

$$k_1(T) = (3.5 \pm 0.8) \cdot 10^{13} (T/295\ \mathrm{K})^{-1.5}\ \mathrm{cm^3/mol\ s}$$

can be explained with the reaction dynamics calculated in (3) by means of *ab initio* molecular orbital theory. The interaction predominantly between the nitrogen and an oxygen lone pair gives rise to the formation of an initial donor-acceptor complex, after which hydrogen migration with a small rearrangement barrier of 27 kJ/mol leads to the more stable tautomer H_2N-OH hydroxylamine (see Fig. 5).

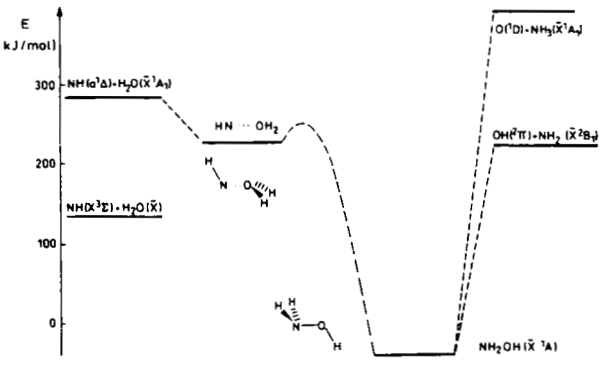

Fig. 5
Correlation diagram of the reaction NH(a) + $H_2O(\tilde{X})$ and dynamics due to the calculations in (2) and (3)

This complex formation gives rise to a negative temperature dependence of k_1. Prior to the decomposition of the donor-acceptor complex no exchange of isotopes takes place whereas the electronic chemically activated hydroxylamine decomposes to the final products $NH_2(\tilde{X}) + OH(X)$.

The reaction dynamics of $NH(X^3\Sigma^-)$ with H_2O:

$$NH(X^3\Sigma^-) + H_2O(\tilde{X}) \rightarrow \text{products}$$

is completely different from that one of reaction (1). It proceeds with a rate constant $k(T) = 2 \cdot 10^{13} \exp(-58\ \text{kJ mol}^{-1}/RT)\ \text{cm}^3/\text{mol s}$. The only reaction products which are exothermic:

$$NH(X) + H_2O(\tilde{X}) \rightarrow HNO(\tilde{X}^1A') + H_2(X^1\Sigma_g^+)$$
$$\Delta_R H = -24.6\ \text{kJ/mol}$$

are spin-forbidden. The abstraction pathway:

$$NH(X) + H_2O(\tilde{X}) \rightarrow NH_2(\tilde{X}) + OH \quad \Delta_R H = +110\ \text{kJ/mol}$$

is so endothermic that it is excluded by the measured activation energy of 58 kJ/mol. The spin-allowed pathway:

$$NH(X^3\Sigma^-) + H_2O(\tilde{X}^1A_1) \rightarrow HNO(\tilde{a}^3A'') + H_2(X^1\Sigma_g^+)$$
$$\Delta_R H = +52\ \text{kJ/mol}$$

the endothermicity of which is not in contradiction with the measured activation energy [14, 15] and one can imagine that these products are formed without an intermediate complex. Thus one can conclude that the multiplicity restrictions give rise to the activation energy in the $NH(X^3\Sigma^-)$ reaction.

The reaction:

$$NH(a) + H_2O_2 \rightarrow \text{products} \qquad (2)$$

was found to be very fast i.e. nearly every gas kinetic collision leads to NH(a) depletion. It has, to our knowledge, not yet been studied directly. Although no theoretical studies are available for this reaction one can assume that the same reaction dynamics occurs as for H_2O. Since there are two O atoms in the molecule one can imagine that the donor-acceptor complex formation is faster than for H_2O.

The vibrational excitation in NH(a) does not accelerate the reaction, which can be interpreted in the same way as the negative temperature dependence of $k_1(T)$. From the fact that k_2'' is slightly smaller than k_2' two things may be concluded. At first that the vibrational quenching pathway:

$$NH(a, v = 1) + H_2O_2 \rightarrow NH(a, v = 0) + H_2O_2$$

is of no importance. Secondly that reaction (2) proceeds via a complex formed without a barrier which the vibrational energy might help to overcome. The high absolute values of k_2 also indicate that the reaction has no activation barrier. As in the case of many other reactions of NH(a) of the type:

$$NH(^1\Delta) + \text{singlet} \longrightarrow \text{doublet} + \text{doublet}$$
$$\not\longrightarrow \text{triplet} + \text{singlet}$$

the quenching is unimportant. Quenching of NH(a) contributes significantly only for reactions of the type

$$NH(^1\Delta) + \text{doublet} \rightarrow \text{triplet} + \text{doublet}$$

like in the reaction of NH(a) with NO.

The formation of $NH_2(\tilde{X})$ observed in this work can be interpreted as a decomposition product of an electronic chemically activated perhydroxylamine:

$$NH(a) + H_2O_2(\tilde{X}) \rightarrow NH_2-O-O-H(\tilde{X})^{\#}$$
$$\rightarrow NH_2(\tilde{X}) + HO_2(\tilde{X})$$
$$\Delta_R H = -191.3\ \text{kJ/mol}$$

Also other spin-allowed reaction channels are exothermic:

$$NH(a) + H_2O_2 \rightarrow H_2NO(\tilde{X}^2A') + OH(X)$$
$$\Delta_R H = -285.5\ \text{kJ/mol}$$
$$\rightarrow NH_3(\tilde{X}) + O_2(a^1\Delta)$$
$$\Delta_R H = -342.4\ \text{kJ/mol}$$

and even the formation of H_2O and NO is exothermic

$$NH(a) + H_2O_2 \rightarrow NO(X^2\Pi) + H_2O(\tilde{X}) + H(^2S)$$
$$\Delta_R H = -323\ \text{kJ/mol}$$

It has to be assumed that at least one of these product channels contribute to the non observed products. The reaction of NH in its electronic ground state with H_2O_2 has not yet been measured directly.

We are greatly indebted to Prof. Dr. H. Gg. Wagner for his generous support and stimulating interest. The financial support of Deutsche Forschungsgemeinschaft (SFB 357) is acknowledged.

References

[1] M. Röhrig and H. Gg. Wagner, 25th Symp. Int. Combust. 975 (1994).
[2] J.A. Pople, K. Raghavachari, M.J. Frisch, J.S. Binkley, and P.R. Schleyer, Am. Chem. Soc. *105*, 6389 (1983).
[3] P.V. Sudhakar and K. Lammertsma, Am. Chem. Soc. *113*, 5219 (1991).
[4] J. Kawai, S. Tsunashima, and S. Sato, Chem. Lett. *6*, 823 (1983).
[5] W. Hack and H. Orthner, Z. Phys. Chem. *188*, 275 (1995).
[6] A. Wilms, PhD thesis, University Göttingen 1987.
[7] A. Schiffman, D.D. Nelson, and D.J. Nesbitt, J. Chem. Phys. *98*, 6935 (1993).
[8] R. Schinke and V. Staemmler, Chem. Phys. Lett. *145*, 487 (1988).
[9] R. Jordan, Dipl. thesis, University Göttingen 1996.
[10] W. Hack and R. Jordan (to be published).

[11] W.B. DeMore, M.J. Molina, S.P. Sander, D.M. Golden, R.F. Hampson, M.J. Kurylo, C.J. Howard, and A.R. Ravishankara, J. Phys. Lett. *87*, 41 (1987).
[12] W. Hack and K. Rathmann, J. Phys. Chem. *96*, 47 (1992).
[13] W. Hack and A. Wilms, Phys. Chem. NF *161*, 107 (1989).
[14] S.P. Walch and C. McMichael Rohlfing, Chem. Phys. *91*, 2939 (1989).
[15] Guadagnini, G.C. Schatz, and S.P. Walch, J. Chem. Phys. *102*, 774 (1995).

Presented at the Discussion Meeting of the Deutsche Bunsen-Gesellschaft für Physikalische Chemie "Unimolecular Reactions" in Tutzing, October 21st to 24th, 1996

E 9472